Iterative reconstruction algorithms in neutron tomography imaging

Gerges M. Salama[1] · Hesham F. A. Hamed[1,2] · Fathi E. Abd El-Samie[3,4] · Imbaby I. Mahmoud[5] · Waleed Abd el Bar[1,6] · Magdy M. Zaky[6]

Abstract For the nondestructive assessment of heavy industrial components and soft hydrogenous materials encased in heavy metals, which are typically challenging to image with X-rays, neutron tomography imaging is a particularly potent tool. Tomography imaging scanner technology has progressed rapidly throughout the past decade, with major advances in neutron computer tomography (NCT) detection system speed and image reconstruction that have resulted in a still-increasing number of novel computer tomography (CT) applications. This paper provides a comprehensive survey of the idea of iterative reconstruction (IR) of radiation dose with noise and artifact reduction. Additionally, the impact of model-based and statistical (hybrid) IR algorithms on image quality is exemplified by comparing them with the conventional filter-based back-projection (FBP) algorithm utilized for image reconstruction in NCT.

✉ Waleed Abd el Bar
  waleed.abdelbar@eaea.sci.eg

1 Department of Electrical Engineering, Faculty of Engineering, Minia University, Minia 61111, Egypt

2 Faculty of Engineering, Egyptian-Russian University, Cairo, Egypt

3 Department of Electronics and Electrical Communications Engineering, Faculty of Electronic Engineering, Menoufia University, Menouf 32952, Egypt

4 Department of Information Technology, College of Computer and Information Sciences, Princess Nourah Bint Abdulrahman University, P.O. Box 84428, 11671 Riyadh, Saudi Arabia

5 Egyptian Atomic Energy Authority, NCRRT, Cairo, Egypt

6 Egyptian Atomic Energy Authority (AEA), ETRR-2, Cairo, Egypt

Introduction

In the industrial sector, neutron computerized tomography (NCT) has been utilized to examine items non-destructively by investigating the interior and exterior of objects. This method is solid for visualizing hydrogenous materials in three dimensions, including wood, rubber, water, oil, explosives, and even layers of thick metal. The primary distinction between X-rays and neutrons in their interaction with matter leads to additional advancements in neutron techniques, such as their heightened sensitivity to light elements and their high matter penetration capabilities. Neutron computerized tomography (NCT) is beneficial in a wide range of fields, including biology, geology, science, archeology, cultural heritage, and industrial applications [1, 2].

A radiation detector (CCD camera) on the opposite side of the object is used to measure the transmission of the neutron image, which is created by irradiating the object with a uniform neutron beam and recording the intensity of radiation it emits. Based on the object cross-section, 2D reconstructed images (projections) are created using the observed radiation. A 3D visualization of the object can then be created by compiling the 2D reconstructed images.

Through the use of mathematics, NCT reconstruction creates tomographic images from projection data that was collected around the sample from different angles using measurable data as an input to compute the output, or density distribution, of the desired cross-section of the sample under investigation. Consequently, it is possible to obtain the desired-cross-section two-dimensional image.

The relevant reconstruction algorithms can be categorized into three groups: back-projection reconstruction, IR, and analytical reconstruction.

It is now feasible to establish software-based methods for IR of CT images thanks to the recent advancements in computing power [3, 4]. The iterative enhancement of observed projected and/or reconstructed image data by the application of filters based on statistical data models or mathematical models of the CT imaging process is the common technological principle of IR algorithms. This contrasts with well-known analytical image reconstruction algorithms like filtered back projection (FBP). Compared to FBP, these IR algorithms enable the simultaneous improvement of overall image quality and the decrease of image noise. Because noise and overall image quality are highly connected with the radiation exposure collection, suppressing or lowering noise through the use of IR algorithms allows for dose reduction [5–7]. The goal of this research work is to supply the research facility with open-source software and data processing techniques for image reconstruction that are both user-friendly and capable of producing the best reconstruction quality.

Materials and methods

The neutron tomography in the ETRR-2

The ETRR-2 NCT facility serves as the location for the actual work. The tomography setup was placed at the ETRR-2 horizontal beam. Figure 1 shows the detection system in the NCT facility, to shelter it from neutrons and gamma rays. The camera and electronic parts are shielded by boron carbide sheets. In a typical tomography system, a mirror, a cooled CCD camera, a computer support depending on Lab View, a neutron scintillation screen, a (ZnS
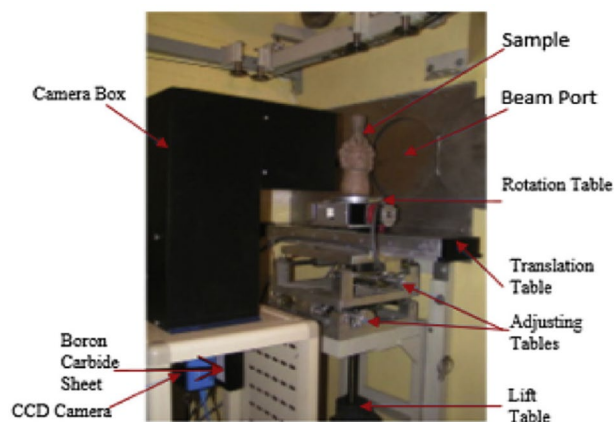

Fig. 1 Neutron imaging system at the ETRR-2 facility

(Ag)–6LiF) rotatable object, and other components, are used to obtain the image. For every projection, the transmitted neutron intensity is received by the scintillator screen, and the created light is reflected by the mirror and recorded by the cooled CCD camera. The light path is 90° bent by the mirror. The object is typically rotated in steps of 0–180° or 360° to obtain the required number of projections [8, 9]. The camera records the light from the scintillator using a 45° mirror to reduce radiation damage to the CCD ships caused by gamma and neutron radiation.

Implementation of CT reconstruction using an iterative algorithm

Before the end product becomes suitable for post-data analysis, a raw dataset in the tomographic reconstruction process passes through several data-processing algorithms [10]. Two fundamental requirements are met by the software: the observed refractive indices are the closest to the calculated values, and the reconstructed images exhibit the fewest artifacts. As shown in Fig. 2, preprocessing, reconstruction, and post-processing are the three phases of the reconstruction procedure. Numerous data processing algorithms can be applied at each step, and they can all operate in various spaces, such as reconstruction, sinogram, and projection. Because the transition between the sonogram and projection spaces necessitates intermediate data storage, preprocessing techniques must be selected to operate in the same area during this stage.

Preprocessing techniques

- Modulation transfer function (MTF)

Because of the scintillation screen scattering, pixel reaction is influenced by the amount of light from its surroundings. If the dispersion of photons is uniform, the linearity assumption remains valid. However, the form of the sample and its absorption properties determine this criterion. We may observe the effect of scintillation scattering quite clearly by examining the interface areas between the sample and the open space of the flat-field-corrected projection. The sample is surrounded by a dark current as a result. By figuring out the scintillator MTF using a calibration image and following the instructions in [11], the loss of resolution brought on by the scintillation screen scattering in a scintillator-based detector system is minimized.

- Flat–field correction

By dividing an image with a sample by an image without a sample or a flat-field image, the intensity ratio of the image

Fig. 2 Three steps of the neutron tomographic reconstruction procedure, where many data processing techniques can be added to the software depending on the projection material and the hardware issues of the NCT system
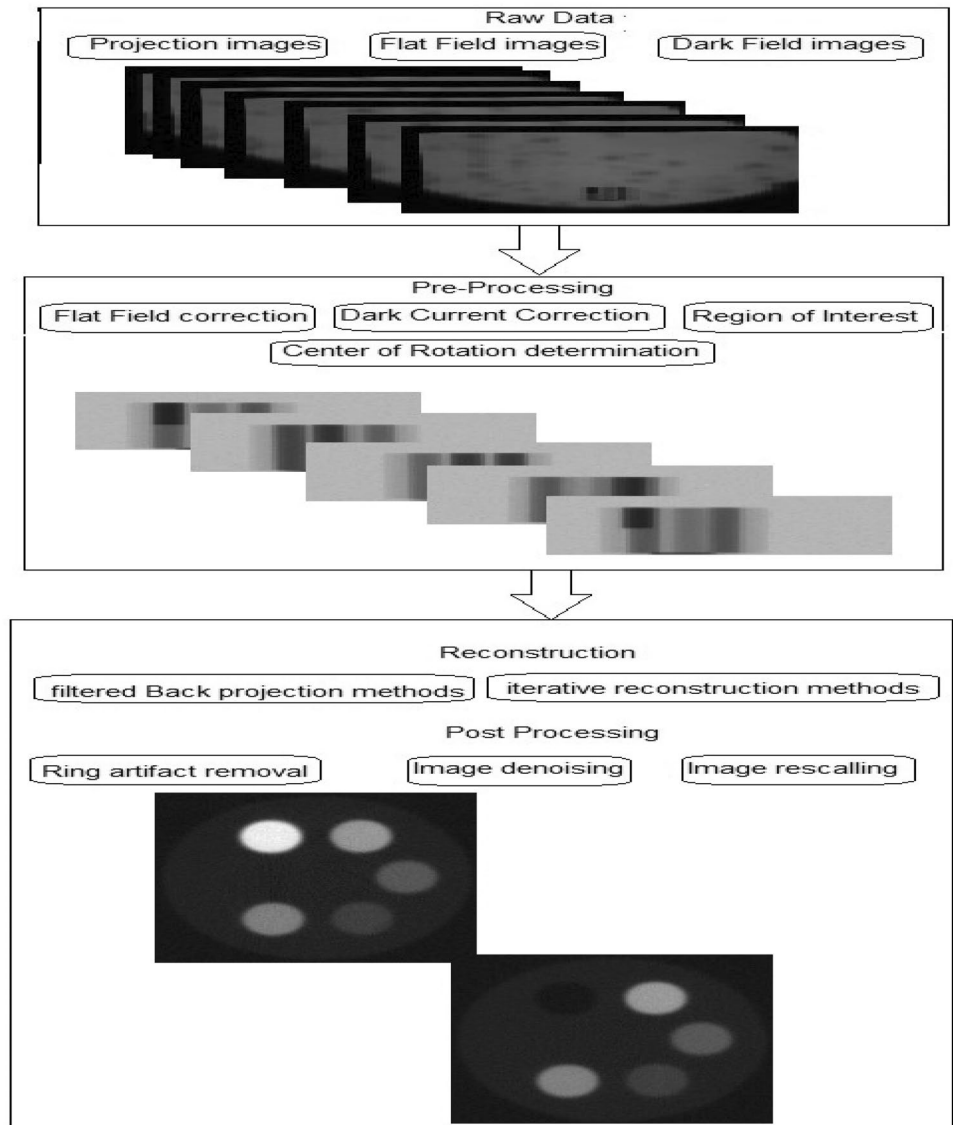
to the incoming beam at each pixel is corrected. A dark-field image is subtracted from each image before the division.

$$\frac{tomography\ image(x,y) - \overline{dark\ current\ image(x,y)}}{open\ beem\ image(x,y) - \overline{dark\ current\ image(x,y)}} \quad (1)$$

Iterative reconstruction (IR) algorithms

A projection model plus back-projection of the error in the projection domain make up the IR algorithm [12]. Reconstruction algorithms that iteratively reduce image noise and artifacts have several benefits. Image quality can be significantly enhanced by using previous knowledge, particularly for sparse or missing data. Given the significant advancements in computer hardware, it is feasible that iterative algorithms find widespread applications.

While the simultaneous iterative reconstruction technique (SIRT) and simultaneous algebraic reconstruction technique (SART) update the rebuilt results by the average error of all rays, the algebraic reconstruction technique (ART) [13] updates the reconstructed results ray per ray. The results of the survey of open-source toolkits for the reconstruction of CT images are summarized in Table 1.

The vector **f** representing the solution of the equation **g = Af** is the target we are looking for. The goal of iterative algorithms is to find a solution through successive approximations. The measured projections and the projections that match the current estimates are contrasted. The current estimate is modified using the comparison

Table 1 Survey of CT image reconstruction open software

Toolkit	Data pre-processing	Post processing	Reconstruction algorithms	Software environment	Year
ASTRA	No	Yes	FBP, SIRT, FDK SART	Windows /Linux: C++/MATLAB/Python	2016
CTsim	No	No	Fourier inverse transformation, FBP	Windows /Linux: C++/GUI	2015
OSCAR	No	No	FDK	Windows: MATLAB/GUI	2008
SNARK14	Yes	NO	FBP, ART, SIRT	Linux: C++/GUI	2019
TIGRE	Yes	Yes	FDK, SART, SIRT	Windows/Linux: C++/MATLAB/Python	2015
TomoPy	Yes	Yes	ART	Windows: C/ Python	2019

outcome to provide a new estimate. The methods vary in how the estimated and measured projections are compared, as well as in the type of adjustment that is performed on the current estimate. The procedure begins with the arbitrary creation of a first estimate, such as a uniform image initialized to either 0 or 1 depending on whether the correction is performed as addition or multiplication. We will begin with the additive form of the ART [14]. The following is the iterative process:

$$f_j^{(k+1)} = f_j^{(k)} + \frac{g_j - \sum_{j=1}^{N} f_{ji}^{(k)}}{N} \quad (2)$$

where $f_j^{(k)}$ and $f_j^{(k+1)}$ are the current and the new estimates, respectively; N is the number of pixels along ray I; $\sum_{j=1}^{N} f_{ji}^{(k)}$ is the sum of counts in the N pixels along ray I for the kth iteration; and g_j is the count that is measured for ray I. Equation 2 shows that the new estimate is found by summing over the present estimate with a correction term, and the estimated projections are subtracted from the measured projections as part of the comparison procedure. It is clear that the correction factor approaches zero, when the current estimates are close to the observed projections. 2×2 image blocks are processed using this algorithm as shown in Fig. 3.

Applying Eq. 2 to the measured projections one at a time yields the solution. The maximum likelihood-expectation maximization (MLEM) and the conjugate gradient (CG) algorithms [16–18] are covered in this paper. The MLEM algorithm criterion is to maximize the likelihood of the reconstructed image, whereas the CG algorithm attempts to minimize the difference between g and A_f. Through optimization, both algorithms determine the best estimate for the solution that satisfies a particular criterion.

Results

The same raw data were reconstructed for three studied samples from the neutron imaging facility in the ETRR-2 that are shown in Fig. 4. Both FBP, SIRT, and SART methods have been considered for comparison as shown in Figs. 5, 6, and 7.

The results of the reconstruction using FBP, SIRT, and SART algorithms are evaluated by image quality assessment measures blindly without the need for a reference image. Naturalness image quality evaluator (NIQE) [19], perception-based image quality evaluator (PIQE) [20, 21], and blind/reference-less image spatial quality evaluator (BRISQUE) have been adopted [22, 23], and results are given in Tables 2, 3, and 4.

The images produced by the FBP algorithm are quite grainy and have a significant amount of noise. When employing an IR algorithm, the image smoothness and noise level are significantly affected.

The results of reconstruction by SIRT, and SART algorithms indicate that high-quality images can be obtained without losing information for the three studied samples with different size.

Conclusions

This paper presented a proposed algorithm for image reconstruction by IR algorithms in neutron tomography imaging. Two image reconstruction algorithms, namely SIRT, and SART were investigated. We showed that reconstruction of small objects can be performed. With the appropriate parameters for 3D image reconstruction, the proposed algorithm can be applied to practical problems
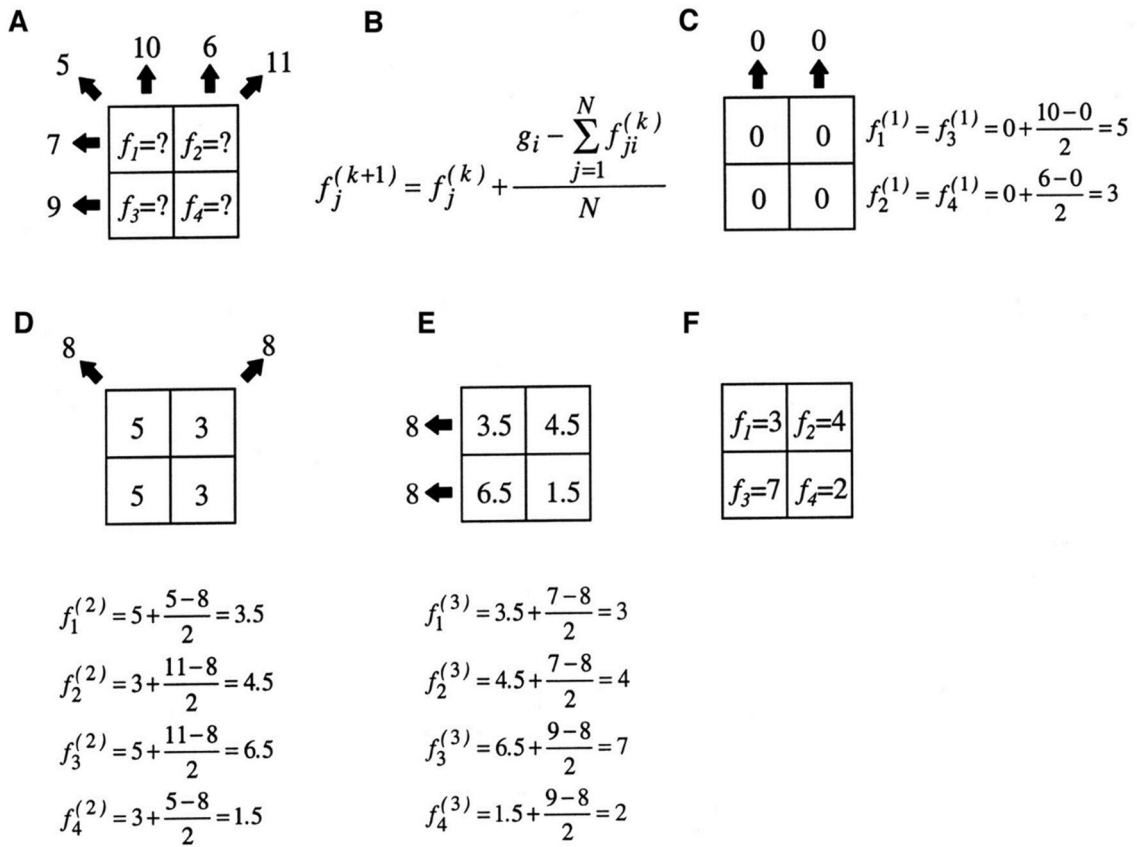
Fig. 3 What do ART algorithms do? **A** The task is to find values for four pixels given values in six bins. **B** ART algorithm: The number of pixels in a given direction is divided by the difference between estimated and measured projections. The outcome is included in the current estimate. **C** Initial action: Apply the ART algorithm, project the original estimate (zeroes) vertically, then update the pixel values. For horizontal **E** and oblique **D** rays, repeat this procedure. **F** After one complete loop, the solution is found. However, more iterations are usually needed for larger images [15]
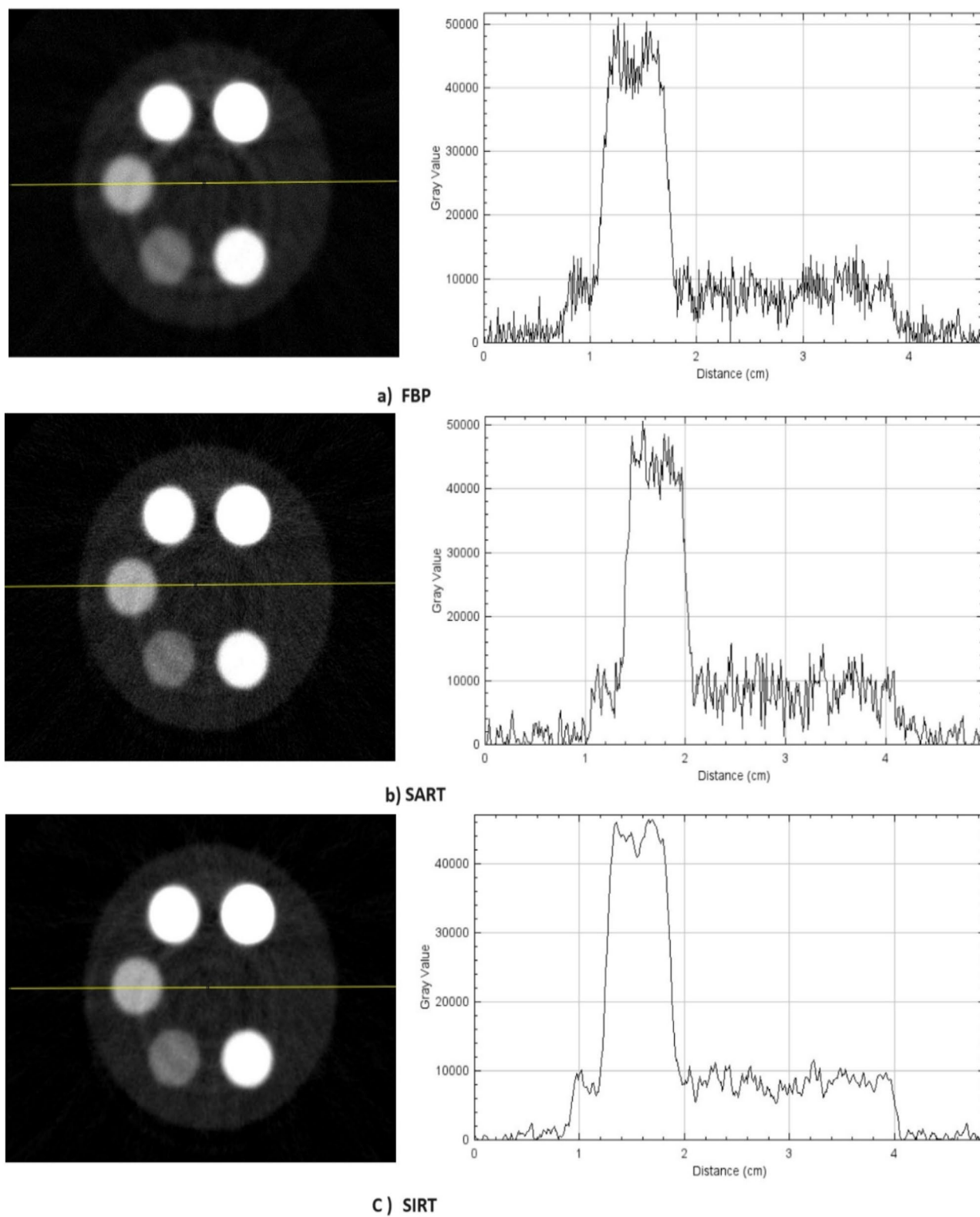

Fig. 4 Studied samples

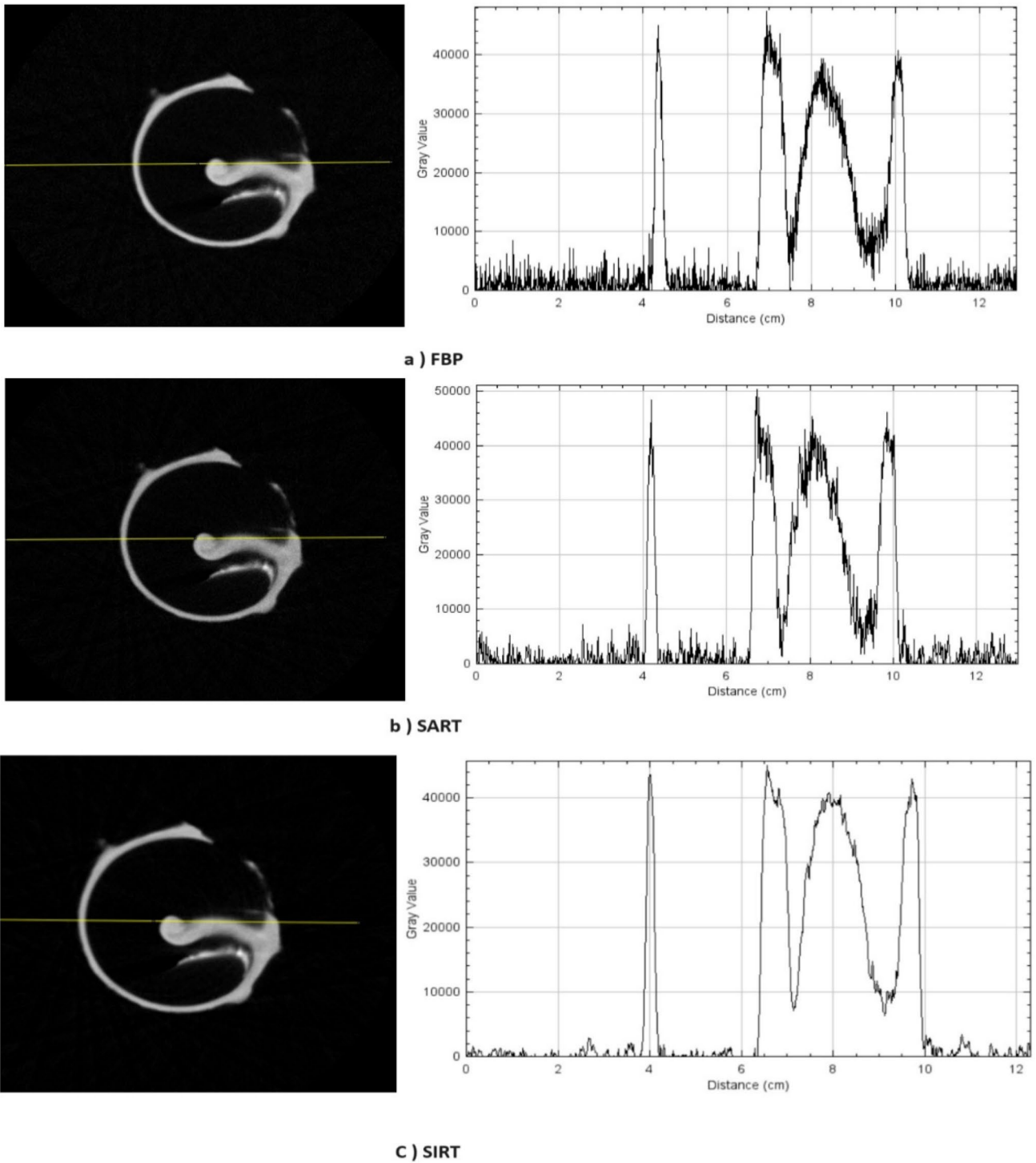**Fig. 5** Contrast CT image reconstruction using different algorithms with line profile for each image

Fig. 6 Sea shell CT image reconstruction using different algorithms with line profile for each image

with larger objects. IR algorithms provide several advantages compared to FBP algorithm as certain algorithms can even enhance low-contrast detection performance, while reducing streak artifacts. The IR algorithm can soon be used widely because of the combination of acceleration algorithms and faster computers.
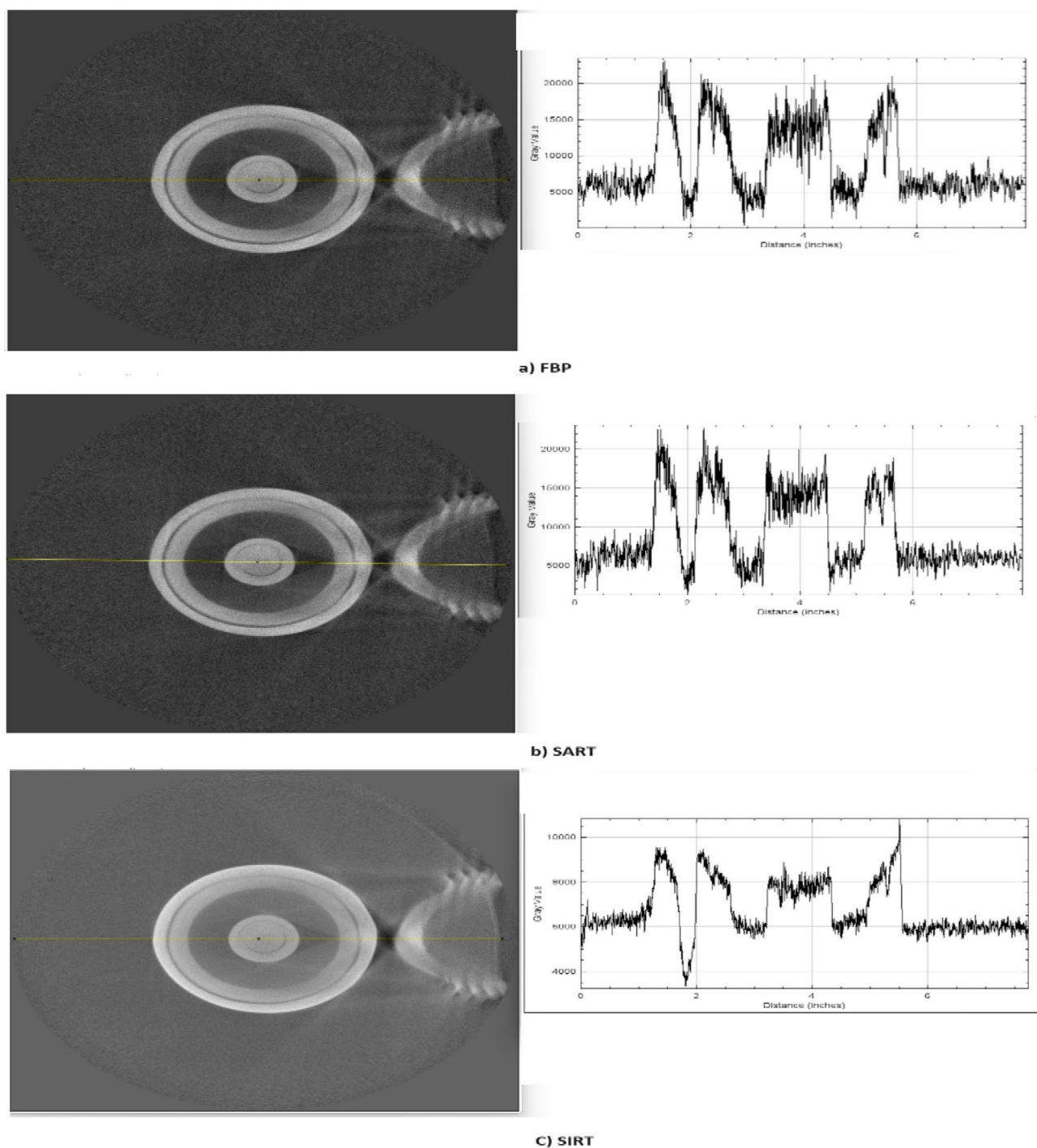
Fig. 7 Fire valve CT image reconstruction using different algorithms with line profile for each image

Table 2 Comparison between reconstructed images for contrast samples using different algorithms

	Mean	Std	RMS	PIQE	NIQE	BRISQUE	entropy
FBP	4740	11,459.9	12,401	74.8619	11.2753	43.4582	4.0437
SART	4508	11,491.7	12,344	57.3533	5.7409	42.6673	3.9603
SIRT	4204	11,491.8	12,236	53.7355	4.1834	46.3295	3.6392

Table 3 Comparison between reconstructed images for the Sea shell using different algorithms

	Mean	Std	RMS	PIQE	NIQE	BRISQUE	Entropy
FBP	2461	6835	7264	75.3369	12.4225	43.4582	3.2863
SART	2240	6930	7284	57.6921	6.4736	43.1502	3.1353
SIRT	1805	6848	7082	62.8114	3.7536	44.5963	2.6883

Table 4 Comparison between reconstructed images for the Fire valve using different algorithms

	Mean	Std	RMS	PIQE	NIQE	BRISQUE	entropy
FBP	7015.16	756.69	6338.46	55.4185	9.3120	48.1698	2.3686
SART	6293.12	779.39	6341.21	27.2337	4.0496	45.8938	2.7195
SIRT	6293.13	766.61	6038.46	23.7519	4.6886	54.6164	4.4530

References

1. R. Nshimirimana et al., X-ray and neutron radiography system optimization by means of a multiobjective approach and a simplified ray-tracing method. J. Nucl. Technol. **207**(1), 147–166 (2021)
2. K.M. Podurets et al., Modern methods of neutron radiography and tomography in studies of the internal structure of objects. Crystallogr. Rep. J. **66**, 254–266 (2021)
3. M.J. Willemink, P.B. Noël, The evolution of image reconstruction for CT-from filtered back projection to artificial intelligence. Eur. Radiol. **29**, 2185–2195 (2019)
4. G.L. Zeng, *Medical Image Reconstruction: A Conceptual Tutorial* (Springer, Berlin, 2010)
5. R.M. Lewitt, Reconstruction algorithms: transform methods. Proc. IEEE **71**(3), 390–408 (1983)
6. P.R. Edholm, G.T. Herman, Linograms in image reconstruction from projections. IEEE Trans. Med. Imaging **6**(4), 301–307 (1987)
7. H. Gao et al., An improved form of linogram algorithm for image reconstruction. IEEE Trans. Nucl. Sci. **55**(1), 552–559 (2008)
8. W. Abd El Bar, I.I. Mahmoud, H.A. Konber, Development and characterization of a neutron tomography system for a research reactor. J. Taibah Univ. Sci. **10**, 195–204 (2016)
9. M.M. Zaky, S. Haggag, W. AbdelBar, T. Mongy, Ageing management of research reactors instrumentation using neutron radiography applications. Alex. Eng. J. **61**, 3229–3235 (2022)
10. R.C. Atwood, A.J. Bodey, S.W.T. Price, M. Basham, M. Drakopoulos, A high-throughput system for high-quality tomographic reconstruction of large datasets at diamond light source. Philos. Trans. A. Math. Phys. Eng. Sci. **373**(2043), 2014039 (2015)
11. N.T. Vo, R.C. Atwood, M. Drak opoulos, Preprocessing techniques for removing artifacts in synchrotron-based tomographic images, in *Proceedings of SPIE 11113, Developments in X-Ray Tomography XII* (2019)
12. Lu. Siyu, Bo. Yang, Ye. Xiao, S. Liu, M. Liu, L. Yin, W. Zheng, Iterative reconstruction of low-dose CT based on differential sparse. Biomed. Signal Process. Control **79**(Part 2), 104–204 (2023)
13. R. Gordon et al., Algebraic reconstruction techniques (ART) for three-dimensional electron microscopy and X-ray photography. J. Theor. Biol. **29**(3), 471–481 (1970)
14. A. Macovski, Tomography, in *Medical Imaging Systems*. ed. by T. Kailath (Prentice-Hall, Englewoods Cliffs,), pp.106–144, (1997)
15. P. Philippe, Bruyant, analytic and iterative reconstruction algorithms in SPECT. J. Nucl. Med. **43**(10), 1343–1358 (2002)
16. W.H. Press, S.A. Teukolski, W.T. Vetterling, B.P. Flannery, Minimization or maximization of functions, in *Numerical Recipes in C*. ed. by W. Press (Cambridge University Press, Cambridge), pp.394–455, (1996)
17. L.A. Shepp, Y. Vardi, Maximum likelihood reconstruction for emission tomography. IEEE Trans. Med. Imaging **1**, 113–122 (1982)
18. L. Kaufman, Maximum likelihood, least squares and penalized least squares for PET. IEEE Trans. Med. Imaging **12**, 200–214 (1993)
19. A. Mittal, R. Soundararajan, A.C. Bovik, Making a "completely blind" image quality analyzer. IEEE Signal Process. Lett. **22**(3), 209–212 (2013)
20. N. Venkatanath, D. Praneeth, B.M. Chandrasekhar, S.S. Channappayya, S.S. Medasani, *Blind Image Quality Evaluation Using Perception Based Features* (IEEE, Piscataway, 2015)
21. H.R. Sheikh, Z. Wang, L. Cormack, A.C. Bovik, *LIVE Image Quality Assessment Database Release 2*. https://live.ece.utexas.edu/research/quality
22. A. Mittal, A.K. Moorthy, A.C. Bovik, Referenceless image spatial quality evaluation engine, in *Presentation at the 45th Asilomar conference on signals, systems and computers*, Pacific Grove, CA (2011)
23. A. Mittal, A.K. Moorthy, A.C. Bovik, No-reference image quality assessment in the spatial domain. IEEE Trans. ImageProcess. **21**(12), 4695–4708 (2012)